Blocking the α4 integrin–paxillin interaction selectively impairs mononuclear leukocyte recruitment to an inflammatory site

Chloé C. Féral,[1] David M. Rose,[1,2] Jaewon Han,[1] Norma Fox,[1] Gregg J. Silverman,[1] Kenneth Kaushansky,[1] and Mark H. Ginsberg[1]

[1]Department of Medicine, University of California San Diego, La Jolla, California, USA. [2]VA San Diego Healthcare System, San Diego, California, USA.

Antagonists to α4 integrin show promise for several autoimmune and inflammatory diseases but may exhibit mechanism-based toxicities. We tested the capacity of blockade of α4 integrin signaling to perturb functions involved in inflammation, while limiting potential adverse effects. We generated and characterized mice bearing a Y991A mutation in α4 integrin [α4(Y991A) mice], which blocks paxillin binding and inhibits α4 integrin signals that support leukocyte migration. In contrast to the embryonic-lethal phenotype of α4 integrin–null mice, mice bearing the α4(Y991A) mutation were viable and fertile; however, they exhibited defective recruitment of mononuclear leukocytes into thioglycollate-induced peritonitis. α4 Integrins are essential for definitive hematopoiesis; however, the α4(Y991A) mice had intact lymphohematopoiesis and, with the exception of reduced Peyer's patches, normal architecture and cellularity of secondary lymphoid tissues. We conclude that interference with α4 integrin signaling can selectively impair mononuclear leukocyte recruitment to sites of inflammation while sparing vital functions of α4 integrins in development and hematopoiesis.

Introduction

Antagonists to α4 integrin are effective in inhibiting a wide variety of experimental models of inflammatory diseases (1–4) and autoimmunity because they inhibit the recruitment of lymphocytes and monocytes to sites of inflammation. Furthermore, anti–α4 integrin antibodies are of proven therapeutic effectiveness in human autoimmune diseases, such as multiple sclerosis (5). Anti–α4 integrin antibodies, such as natalizumab, and small-molecule and peptidomimetic α4 integrin antagonists inhibit the integrin's interactions with ligands such as VCAM-1. At saturation, this form of inhibition causes complete loss of α4 integrin function. Consequently, use of these agents recapitulates the null phenotype, implying the potential for mechanism-based toxicities such as defects in placentation, heart development, and hematopoiesis (6). Furthermore, the blockade of T cell entry into the central nervous system may account for the occurrence of progressive multifocal leukoencephalopathy in humans treated with anti–α4 integrin antibodies (7).

Integrin functions depend on their capacity to generate and respond to cellular signals. Blockade of integrin signaling can leave ligand binding function intact (8–10). Consequently, only partial inhibition of function may occur, even with full blockade of the target, potentially providing a more favorable therapeutic window. A quest for interactions important in α4 integrin signaling uncovered a tight binding interaction of the α4 integrin cytoplasmic domain with paxillin, a signaling adaptor (11). Blocking the interaction by mutations of α4 integrin [e.g., α4(Y991A)] that selectively block paxillin binding, reduces cell migration (10, 11). Furthermore, inhibition of paxillin binding to α4 integrin by a fragment of paxillin (12) or a small-molecule antagonist (13) also impairs migration, suggesting that such agents could be used as therapeutic inhibitors of α4 integrin function. Notably, blocking the interaction of α4 integrin with paxillin does not disrupt α4 integrin–mediated static adhesion (8, 11), suggesting that this form of antagonism might not interfere with functions such as anchorage of hematopoietic progenitors in the bone marrow. We tested this idea by generating mice homozygous for an α4 integrin mutation [α4(Y991A)] that selectively (11) blocks paxillin binding. Here we report that unlike α4 integrin–null mice (6, 14), these mice were viable and fertile; however, they manifested a profound deficit in the recruitment of mononuclear leukocytes to an inflammatory site with no defect in neutrophil recruitment. Furthermore, α4 integrins are essential for definitive hematopoiesis (6, 15, 16); however, the α4(Y991A) mice exhibited normal hemograms, normal abundance of hematopoietic precursors, and unimpaired homing of hematopoietic progenitor cells to the bone marrow, a surrogate marker of stem cell migration. Thus we established the principle that blockade of α4 integrin signaling can impair mononuclear leukocyte recruitment to an inflammatory site while averting the adverse effects of α4 integrin loss on development and hematopoiesis.

Results

Generation of mice bearing the α4(Y991A) mutation. To investigate the role(s) of α4 integrin interaction with paxillin in α4 integrin–mediated functions in vivo, we generated and analyzed mice bearing a point mutation in the α4 integrin tail (Y991A) that inhibits paxillin binding with little detectable effect on the binding of other proteins (11). A targeting vector, α4-pFloxIII, was constructed using the pFloxIII vector (Figure 1A). The Y991A mutation was introduced by PCR into exon 28 in conjunction with an additional silent mutation that creates a unique restriction site, *Eco47III*. Homologous recombinant ES clones (Figure 1B) were then transfected with pTurboCRE vector to remove the selectable markers. Three clones containing the targeted allele were obtained (Figure 1C). Chimeric mice were generated by injection of targeted ES cell clones into C57BL/6-derived blastocysts by standard approaches. Two independent lines were gen-

Nonstandard abbreviations used: BFU-E, erythropoietic burst-forming unit; CFU-Mk, megakaryocyte CFU; Neo, neomycin; TK, thymidine kinase.

Conflict of interest: The authors have declared that no conflict of interest exists.

Citation for this article: *J. Clin. Invest.* doi:10.1172/JCI26091.

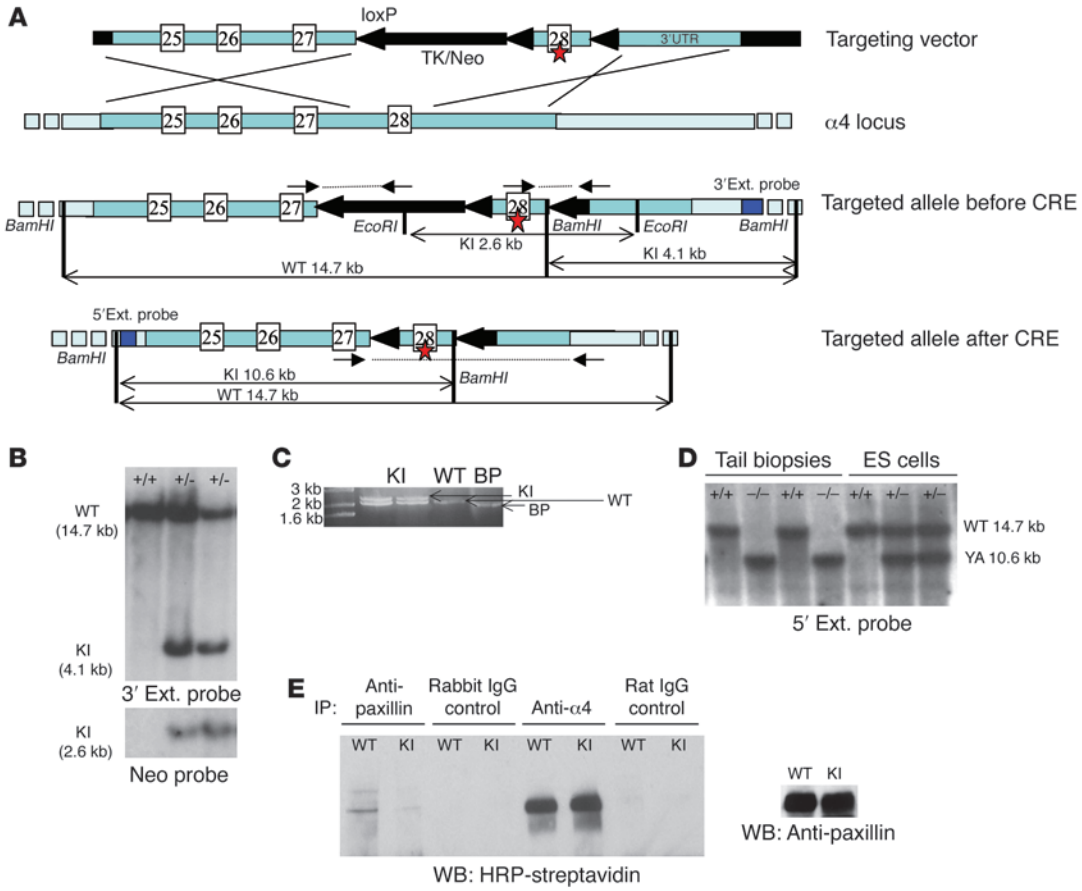

Figure 1

Generation of α4(Y991A) mice. (**A**) Representation of targeting vector, WT α4 locus, and the targeted allele before and after CRE recombination (see Methods for details). The tyrosine 991 (star) was mutated into an alanine, along with the creation of a unique restriction site for *Eco47III*. (**B**) Southern blot analysis of genomic DNA showing correct targeting of the α4 allele. Genomic DNA was isolated from R1 ES cells, digested with *BamHI*, and hybridized with the 3′ probe. Probing the same Southern blot with a specific probe for Neo revealed 1 targeted band at the expected size, indicating that there was a single homologous recombination event. (**C**) PCR analysis of genomic DNA following CRE recombination. Two types of recombination occurred, either between the 2 most external loxP sites (by-product; BP) knocking out both the selection cassette and exon 28, or between the loxP sites flanking the selection cassette (knock-in; KI), selectively removing the cassette. Knock-in clones were subsequently used for blastocyst injection. (**D**) Southern blot analysis of mouse tail genomic DNA showing correct targeting of the α4 allele. Two lines were obtained. WT, heterozygotes, and homozygotes were confirmed by Southern blot using *BamHI*-digested DNA and hybridizing with the 5′ external probe. Targeted band at the expected size [α4(Y991A) (YA), 10.6 kb; WT, 14.7 kb] was obtained. (**E**) Coimmunoprecipitation of α4 integrin with paxillin. Paxillin was immunoprecipitated, and coimmunoprecipitated α4 integrin was visualized by blotting for biotin after separation in SDS-PAGE gel. Immunoprecipitated paxillin was detected by anti-paxillin antibody.

erated, and both manifested the phenotypes described below. Integrin α4(Y991A) heterozygote intercrosses produced viable α4(Y991A) homozygote offspring, as identified by Southern blot analysis (Figure 1D). Heterozygotes were backcrossed on the C57BL/6 line, and the experiments presented in this study were performed on mice from the fifth generation. Viable homozygotes were obtained from both lines. To directly confirm the effect of the α4(Y991A) mutation on primary cells, we isolated T lymphocytes from α4(Y991A) knock-in mice and WT littermates and immunoprecipitated paxillin from these cells (Figure 1E). In paxillin immunoprecipitates from WT cells α4 integrin was present, but it was not detected in those formed from α4(Y991A) cells. The homozygous α4(Y991A) mice were born in Mendelian ratios. These animals were monitored for over 18 months for weight, fertility, and behavior and periodically sacrificed for histological evaluation. Importantly, no major defect was observed, including in the histology of their hearts.

Impaired mononuclear leukocyte recruitment to an inflammatory site in α4(Y991A) mice. To directly test the role of the α4 integrin–paxillin interaction in leukocyte recruitment in vivo, mice were injected with thioglycollate intraperitoneally to induce inflammation. The α4(Y991A) mice exhibited negligible lymphocyte recruitment into the peritoneum. In contrast, WT littermates showed a 3-fold increase in peritoneal lymphocytes 48 hours after the challenge (Figure 2A). Importantly, the α4(Y991A) mice showed no change in peritoneal lymphocytes over a 72-hour period, suggesting a lack of rather than a change in the timing of the peritoneal lymphocytosis in these mice. A delay in early accumulation of monocytes/macrophages was also observed in α4(Y991A) mice (Figure 2B). Importantly, α4(Y991A) mice exhibited a slight monocytopenia (Table 1); however, at 24 hours there was a doubling of peritoneal monocytes/macrophages in WT animals that was lacking in the α4(Y991A) mice, suggesting that lack of monocytes at this time

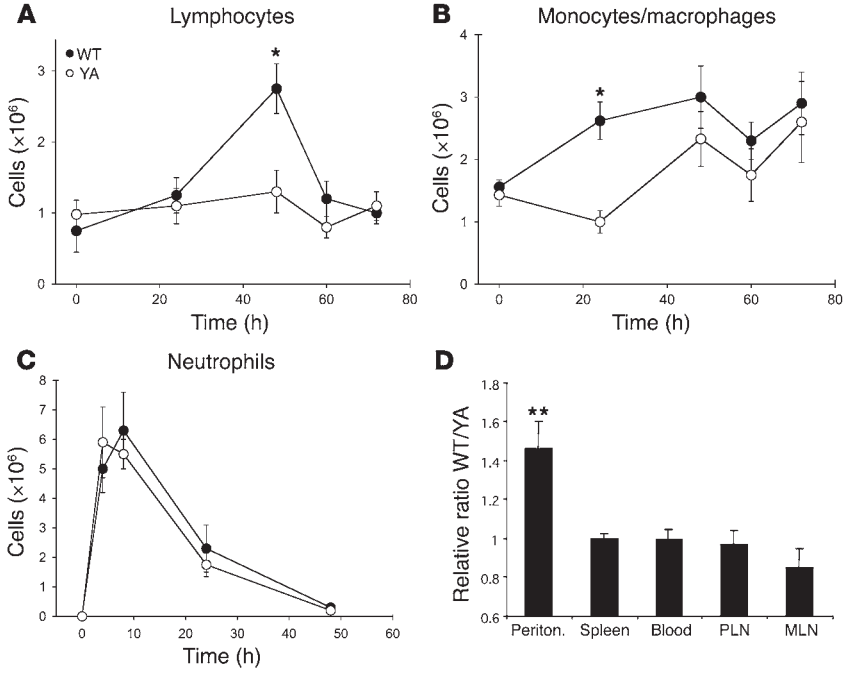

Figure 2
The recruitment of mononuclear leukocytes to the peritoneum in response to thioglycollate is impaired in mice with disrupted α4 integrin-paxillin interaction. (**A**–**C**) WT and α4(Y991A) mice were injected intraperitoneally with thioglycollate, and peritoneal lavage fluid collected at the indicated time points. Total cell number in the lavage fluid was measured with a hemocytometer, and differential cell counts were performed on cytospin slides after modified Wright-Giemsa staining. Results are shown for total lymphocyte (**A**), monocyte/macrophage (**B**), and neutrophil (**C**) counts. *P = 0.013, 2-tailed Student's t test. Results are mean ± SEM of 4–8 mice for each time point. (**D**) Ratios of adoptively transferred WT/α4(Y991A) splenic lymphocytes found in the spleen, blood, peripheral LN (PLN), mesenteric LN (MLN), and thioglycollate-induced inflamed peritoneal cavities (Periton.) of recipient WT mice. Ratios of differentially labeled cells were assessed by flow cytometry and normalized to the starting input ratio. Results are mean ± SEM of 8 mice from 3 separate experiments. **P = 0.037, WT vs. α4(Y991A), 1-tailed Student's t test.

point was ascribable to a defect in recruitment. The impaired recruitment was not true of all leukocyte populations, as both WT and α4(Y991A) mice exhibited similar neutrophil recruitment in response to thioglycollate (Figure 2C). Consequently, we concluded that disruption of the α4 integrin–paxillin interaction results in an impairment in the accumulation of lymphocytes and monocytes but not neutrophils at a site of experimental peritonitis.

To learn whether the defect in peritoneal lymphocytosis was ascribable to defective homing of the mutant leukocytes, we performed mixed adoptive transfer experiments. Splenic mononuclear cells isolated from WT and α4(Y991A) mice were differentially labeled with CFSE and (5/6-[4-chloromethylbenzoyl] aminotetramethylrhodamine), respectively, and injected into recipient WT mice with thioglycollate-induced peritonitis. After 24 hours the relative proportion of transferred WT to α4(Y991A) cells found in the spleen, blood, peripheral and mesenteric lymph nodes, and peritoneal cavity was evaluated by flow cytometry. While the ratio of cells found in the spleen, blood, and peripheral and mesenteric nodes was the same as initially transferred, a significantly higher proportion of WT cells were found in the inflamed peritoneal cavity (Figure 2D). These results demonstrate a selective requirement for the α4 integrin–paxillin interaction in recruitment of mononuclear leukocytes to a site of inflammation, but not for trafficking to several secondary lymphoid tissues.

We next examined potential differences between lymphocyte subpopulations that accumulated in the peritoneum during the course of inflammation. We found that α4(Y991A) mice had less accumulation of both B and T cells than did WT mice, but that the difference was more pronounced in B cells (Figure 3, A and B). To determine whether the reduced B cell numbers were due to a failure of resident B1 cell proliferation or failed peripheral B2 cell influx, we distinguished between these 2 B cell populations in the peritoneum by flow cytometry using $B220^+Mac\text{-}1^+$ and $B220^+Mac\text{-}1^-$ as a marker of B1 and B2 cells, respectively. No significant difference in the number of B1 cells was observed in the peritoneum of WT and α4(Y991A) mice (Figure 3C). However, the dramatic increase in B2 cells in the WT mice was not seen in the α4(Y991A) mice (Figure 3D), demonstrating a failed recruitment of B2 cells from the circulation.

Adequate hematopoiesis in mice with disruption of the α4 integrin–paxillin interaction. Although α4 integrins are implicated in definitive hematopoiesis, this involvement is often age- and cell lineage–dependent. Peripheral blood from α4(Y991A) mice revealed mild monocytopenia (Figure 4A). Otherwise all forms of mature blood cells from the erythroid, myeloid, and lymphoid lineages were present at normal abundance (Table 1). We assessed several additional parameters of hematopoiesis. Marrow cellularity was indistin-

Table 1
Hemograms from WT and α4(Y991A) mice

	WT		α4(Y991A)	
Variable	**Mean**	**SEM**	**Mean**	**SEM**
wbc (×10⁹/l)	2.54	0.26	2.57	0.4
Neutrophils (×10⁹/l)	1030	122	1149	221
Lymphocytes (×10⁹/l)	1167.3	239.9	1181.8	227.3
Monocytes (×10⁹/l)	231.6	27.9	130.0[A]	31.6
Eosinophils (×10⁹/l)	100	34.3	111	24.1
Basphils (×10⁹/l)	0	0	0	0
Erythrocytes (×10⁹/l)	7.5	0.24	7.67	0.31
MCV (fl)	47.3	1.51	45.8	1.24
MCH (pg)	15.2	0.59	14.6	0.43
MCHC (%)	32.26	1.45	31.98	0.91
Hemoglobin (g/l)	114	6.5	112	4.5
Hemacrit (%)	35.3	1.1	35.1	1.3
Platelets (×10⁹/l)	614	67.7	614	66.9

Peripheral blood was collected from the retro-orbital sinus of mice 8–15 weeks old. Cell counts were performed using an automated cell counter with veterinary parameters and reagents. Differential counts were performed manually on Wright-Giemsa–stained smears. MCV, mean corpuscular volume; MCH, mean corpuscular hemoglobin; MCHC, mean corpuscular hemoglobin concentration. n = 6 mice. [A]P < 0.05 vs. WT.

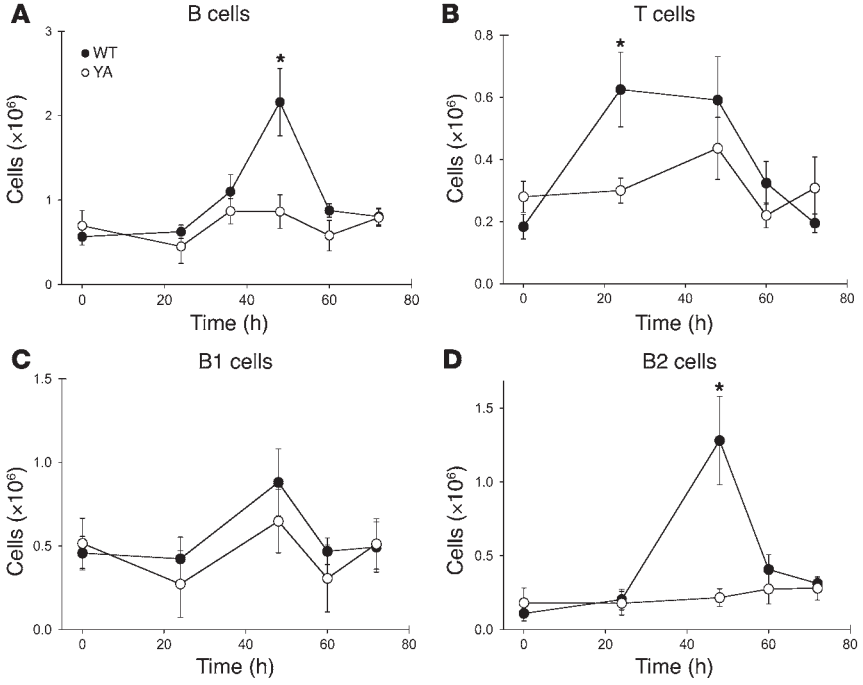

Figure 3
Impaired recruitment of T and B2 cells during thioglycollate-induced peritonitis in mice with disruption of the α4 integrin–paxillin interaction. (**A**–**D**) Peritoneal cells collected as described in Figure 2 were subjected to flow cytometric analysis to distinguish total B cells (**A**), T cells (**B**), B1 cells (**C**), and B2 cells (**D**). The number of T and B cells in lavage fluid was calculated from total lymphocyte counts corrected for the relative percentage of T and B cells determined by flow cytometry staining with B220-PerCP (B cell marker) and CD3-FITC (T cell marker). B1 and B2 subpopulations were distinguished as being B220-PerCP$^+$Mac-1$^-$APC$^+$ and B220-PerCp$^+$Mac-1$^-$APC$^-$, respectively. Results are mean ± SEM of 4 mice for each time point. *$P < 0.05$, 2-tailed Student's *t* test.

guishable between the 2 strains of mice (data not shown). We next assessed the number of erythroid, myeloid, and megakaryocytic progenitor cells in the marrow and spleens of the mice; in 3 independent experiments, the number of erythropoietic burst-forming unit (BFU-E), GM-CFU, and megakaryocyte CFU (CFU-Mk) colonies that developed was no different using marrow cells from α4(Y991A) mice than with controls (Figure 4B). Finally, because integrins are vital for stem cell homing (15), we assessed the ability of bone marrow cells from the 2 strains of mice to home to the marrow and spleens of lethally irradiated normal recipients. Previous studies have shown that homing of GM-CFU to be an excellent surrogate for stem cell homing (17, 18). When marrow cells from α4(Y991A) and normal mice were injected into recipients, the number of GM-CFUs that lodged in the spleen and marrow of recipient mice was similar (Figure 4C).

Lymphopoiesis was examined, as studies from α4 integrin–null chimeric mice suggest the involvement of α4 integrins in both T and B cell development (6, 16). In the bone marrow, pro-B cells (B220$^+$CD43$^+$), pre-B cells (B220$^+$IgM$^-$IgD$^-$), and immature B cells (B220$^+$IgM$^+$IgD$^-$) were found in similar proportions in the WT and α4(Y991A) mice (Figure 5A), which suggests that the α4 integrin–paxillin interaction is not needed for B cell development in the bone marrow. So, too, in the thymus of WT and α4(Y991A) mice, similar numbers of thymocytes transiting the developmental program from CD4$^-$CD8$^-$ to CD4$^+$CD8$^+$, as well as single CD4$^+$ and CD8$^+$ thymocytes, were seen (Figure 5B). Thus the α4 integrin–paxillin interaction is not required for lymphopoiesis in primary lymphoid organs.

In the periphery, the spleens of α4(Y991A) mice had normal architecture of red and white pulp (Figure 6A, top). Splenic follicles of α4(Y991A) mice also had normal structure, with a popu-

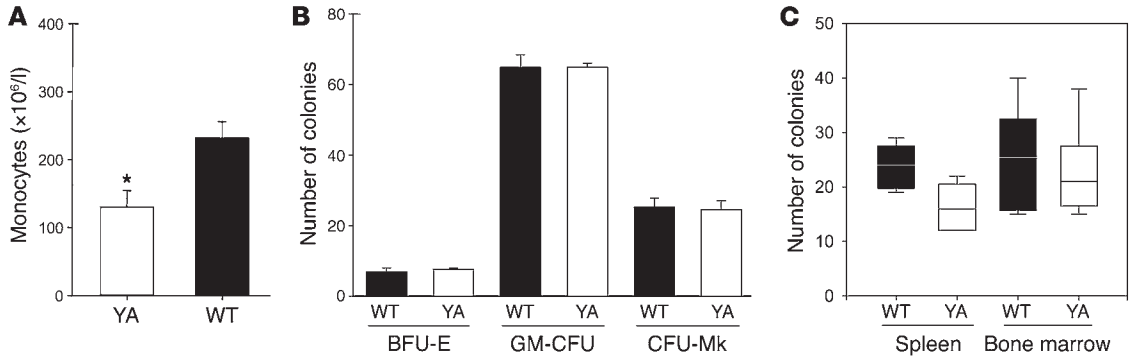

Figure 4
Hematopoiesis in WT and α4(Y991A) mice. (**A**) Peripheral blood monocyte counts are shown, the only blood cell type that displayed a statistically significant difference between the 2 strains of mice. *$P = 0.041$, 2-tailed Student's *t* test. (**B**) The number of BFU-E–, GM-CFU–, and CFU-Mk–derived colonies from WT and α4(Y991A) mice is shown as the mean ± SEM of colonies of each type obtained from 1×10^5 marrow cells from each of 4 mice. A representative example of 3 separate experiments giving essentially identical results is shown. The mean number of colony-forming cells was not statistically different (Student's *t* test). (**C**) The number of GM-CFU derived from the marrow or spleens of lethally irradiated recipient mice following intraocular injection of 2×10^7 marrow cells is shown; the data shown represent the mean ± SEM of results from 4 mice in each group. The number of progenitors that lodged in the marrow (per 1×10^5 cells plated) and spleens (per 2×10^5 cells plated) was not significantly different (2-tailed Student's *t* test).

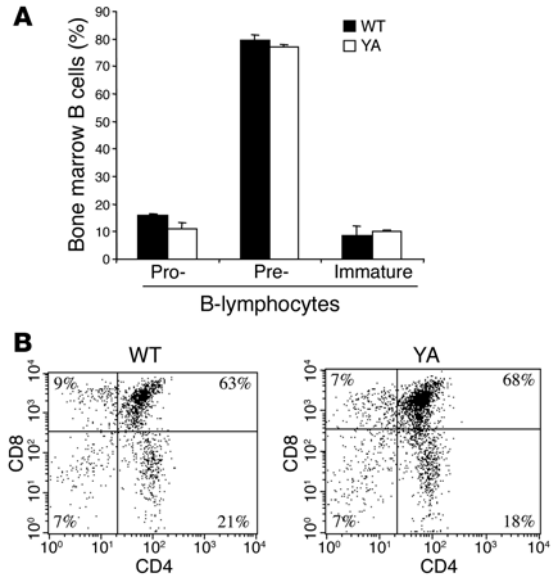

Figure 5
Disruption of the α4 integrin–paxillin interaction does not interfere with T and B cell development in primary lymphoid organs. (**A**) The relative percentage of B220$^+$ pro-, pre-, and immature B lymphocytes from bone marrow isolated from WT and α4(Y991A) mice between 6 and 8 weeks of age is shown. Flow cytometry was used to distinguish pro-B cells (B220$^+$CD43$^+$), pre-B cells (B220$^+$IgM$^-$IgD$^-$), and immature B cells (B220$^+$IgM$^+$IgD$^-$). Results are mean ± SEM from 6–8 mice. (**B**) The percentage of thymocytes expressing CD4/CD8 is shown. Thymocytes were collected from WT and α4(Y991A) mice and analyzed for CD4 and CD8 expression by flow cytometry. Results are representative of 6–8 different mice.

lation of macrophages separating marginal zone B cells from follicular B cells (Figure 6A, bottom), and similar proportions of T and B cells were observed in WT and α4(Y991A) mice (Figure 6B). As α4β1 has been implicated in B cell retention in the marginal zone of germinal centers (19, 20), we analyzed the abundance of marginal zone B cells by flow cytometry and histology. Marginal zone B cells (CD21/35$^+$CD23$^-$) were found in similar proportion relative to follicular B cells (CD21/35$^+$CD23$^+$) in both WT and mutant mice (Figure 6C). On histology, the marginal zone B cells (IgM$^+$IgD$^-$) were present as a distinctive ring around the follicles in both WT and α4(Y991A) mice (Figure 6D).

Adequate humoral immune response in mice with disruption of α4 integrin–paxillin interaction. The strongest effect of the α4(Y991A) mutation was on B cell trafficking, suggesting that it might impair the capacity to mount a protective humoral immune response. The effective lymphopoeisis and normal structure and cellularity of secondary lymphoid tissues in α4(Y991A) mice suggested that humoral immunity would be intact. To test this idea further, WT and α4(Y991A) mice were immunized with T cell–dependent (TNP-KLH) and T cell–independent type I (TNP-LPS) and type II (TNP-Ficoll) antigens. Similar levels of anti-TNP IgM were generated in α4(Y991A) and WT mice in response to TNP-KLH, suggesting adequate follicle B cell function (Figure 7). Furthermore, the equivalent generation of specific IgG observed in these mice indicates that isotype switching is not impaired by disrupting the α4 integrin–paxillin interaction. Similarly, α4(Y991A) mice responded equally well as WT mice to TNP-LPS and TNP-Ficoll, suggesting adequate function of the marginal zone and/or B1 cells (Figure 7). Collectively, these data indicate that α4 integrin–paxillin interaction is not required to mount a humoral immune response, and therefore disrupting the interaction does not impair this aspect of host defense.

Altered formation of Peyer's patches in mice with disruption of the α4 integrin–paxillin interaction. Peyer's patches in the gut were examined, as α4 integrins play roles in both their formation and subsequent population with T and B lymphocytes (6). We found α4(Y991A) mice had significantly fewer Peyer's patches than did WT mice (Figure 8A). However, these Peyer's patches were of similar size, cellularity, and histological appearance as those seen in WT mice (Figure 8, B and C). Furthermore, the relative proportion of T and B cells in the Peyer's patches was not different between WT and α4(Y991A) mice (Figure 8D). These results suggest that the α4 integrin–paxillin interaction plays a role in early Peyer's patch formation, but not in the homing to the Peyer's patches, of lymphocytes involved in mucosal immunity.

Discussion

The promise of integrin-directed therapeutics has been limited by mechanism-based toxicities that constrict the therapeutic window. In the present work, we have validated interference with integrin signaling as a means to selectively perturb integrin functions involved in inflammation while limiting mechanism-based toxicity. We generated mice bearing the α4(Y991A) mutation and established that the mutation disrupts α4 integrin–paxillin interaction in primary mouse lymphocytes. In contrast to the embryonic lethal phenotype of the α4 integrin–null mouse (14) or to the impairment in hematopoietic stem and progenitor cell homing and expansion in mice bearing α4 integrin–null mutations in their hematopoietic cells (15), mice bearing the α4(Y991A) mutation were viable with no gross abnormalities in placental, hematopoietic, or cardiac development. However, these mice exhibited a profound defect in the recruitment of mononuclear leukocytes into a site of inflammation. Furthermore, there was little impairment of lymphohematopoiesis caused by disruption of the α4 integrin–paxillin interaction in these mice. With the notable exception of a reduction in the number of Peyer's patches, the architecture and cellularity of secondary lymphoid tissues was not greatly affected by the α4(Y991A) mutation, and no impairment in T cell–dependent and –independent humoral immune responses was evident. Furthermore, no gross defects were observed in the size of the Peyer's patches or in the proportion of T and B cells in the spleen. These results validate the concept that interference with integrin signaling can selectively impair lymphocyte recruitment to sites of inflammation while sparing vital functions of α4 integrins in development, hematopoiesis, and humoral immunity.

The α4(Y991A) mutant disrupted the interaction of α4 integrin with paxillin in primary cells but did not cause embryonic lethality. Mutant α4 integrin–null mice develop placental failure due to the failure of the chorion and allantois to fuse (14). However, we found no evidence of fetal wastage in the α4(Y991A) homozygotes, even when they were borne by homozygous mothers. In cardiac development, attachment of the epicardium to the underlying myocardium is also lost in α4 integrin–null mice (14, 21). Detailed analysis of cardiac histology at 6 weeks of age revealed normal-sized hearts, with no evidence of myocardial fibrosis, myocyte loss, or inflammatory infiltrates. However, abnormalities of cardiac

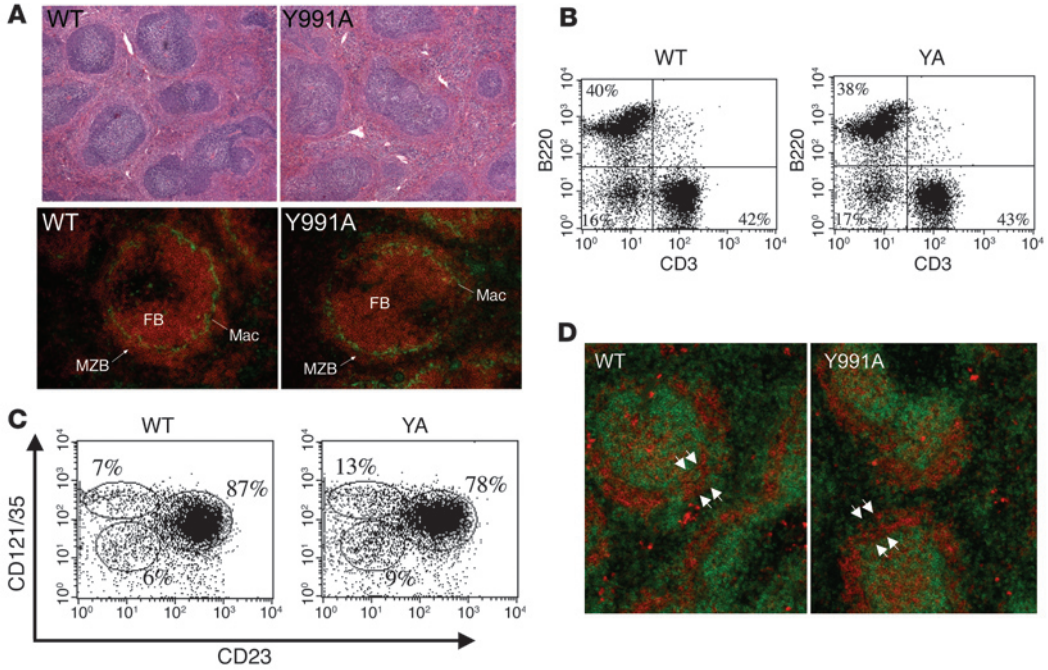

Figure 6

The α4 integrin–paxillin interaction is not required for normal architecture and lymphocyte distribution within the spleen. (**A**) Histology of spleens from WT and α4(Y991A) is shown. Sections from paraffin embedded spleens were stained with H&E. Immunofluorescence of splenic sections stained with MOMA-1 (green) to detect macrophages and B220 (red) to detect B cells is also shown. The locations of macrophages (Mac), follicular B cells (FB), and marginal zone B (MZB) cells are indicated. (**B**) The relative percentage of T and B cells in the spleen is shown. Splenocytes from WT and α4(Y991A) mice were analyzed by flow cytometry for CD3 (T cell marker) and B220 (B cell marker). (**C**) The relative percentage of B cell subpopulations in the spleen is shown. Cells were stained for B220, CD21/35, and CD23, and flow cytometry was used to distinguish marginal zone B cells ($CD21/35^+CD23^-$), follicular B cells ($CD21/35^+CD23^+$), and immature B cells ($CD21/35^-CD23^-$). (**D**) Follicular architecture in spleens from WT and α4(Y991A) mice. Immunofluorescence of tissue sections was performed with anti-IgM (red) and anti-IgD (green) to distinguish the position of B cell follicles with a rim of marginal zone B cells (IgM^+IgD^-). Arrows indicate the marginal zone around the follicle. Results are representative of 6–8 different mice. Magnification, ×4 (**A**, top); ×20 (**A**, bottom, and **D**).

function sometimes require stress to become manifest; it will be of interest to perform such studies on the α4(Y991A) mice.

In vitro, the α4 integrin–paxillin interaction is not required for α4β1 integrin–dependent static cell adhesion (8, 11). Since placentation and cardiac development involve α4 integrin–mediated adhesion of tissue layers (14, 21), this preservation of adhesive function may account for the normal heart and placental development. However, α4β1-dependent cell migration of epicardial progenitors has been implicated in formation of the epicardium (21). These results raise the fascinating possibility that the paxillin dependence of α4 integrin–mediated migration may be cell type–specific. Alternatively, expression of α9, a paralog of α4, during development could also complement some of the migration deficits in the α4(Y991A) mice (22). In sum, the α4(Y991A) mutation that blocks lymphocyte migration lacks the severe developmental phenotypes associated with lack of α4.

The α4 integrin–paxillin interaction is important in Peyer's patch organogenesis but not in its subsequent population with lymphocytes. The α4(Y991A) knock-in mice had approximately 30% fewer Peyer's patches than did WT littermates, similar to the reductions seen in mice treated with function-blocking antibodies to α4 integrin or VCAM-1 (23). Peyer's patch formation involves the interaction of α4β1-expressing $CD4^+CD3^-$ hematopoietic cells and VCAM-1–expressing intestinal stromal cells. The interaction is dependent on CXCR5-induced α4β1 activation, as measured by binding of β1 integrin with 9EG7 antibody (23, 24). Hyduk et al. have reported that paxillin selectively associates with activated high-affinity α4β1 (25). Thus the impairment of the α4 integrin–paxillin interaction may prevent the activation-dependent interaction of hematopoietic cells with intestinal stromal cells. Importantly, the Peyer's patches that formed were of normal size and cellularity, in contrast to the reduced cellularity seen with α4 integrin–null lymphocytes. Thus our results highlight differential requirements for α4 integrin signaling in the formation and subsequent population of Peyer's patches.

The present study suggests that antagonists that target integrin signaling could overcome some of the mechanism-based toxicities that limit integrin-directed therapies. For example, αIIbβ3 antagonists completely block platelet aggregation leading to their remarkable efficacy in preventing acute thrombosis (26). However, the need to limit dosage to avoid bleeding was a major factor in the failure of chronic oral therapy with these agents. Similarly, α4 integrin antagonists block T cell entry into inflammatory sites in the brain, a property that made them a promising new therapy for multiple sclerosis (1). However, blockade of T cell surveillance in the brain may underlie their association with progressive multifocal leukoencephalopathy (7). Here we have shown that interfering with α4 integrin signaling blocked lymphocyte recruitment to sites of inflammation with little effect on lymphohematopoiesis, lymphocyte homing to several secondary lymphoid organs, or the

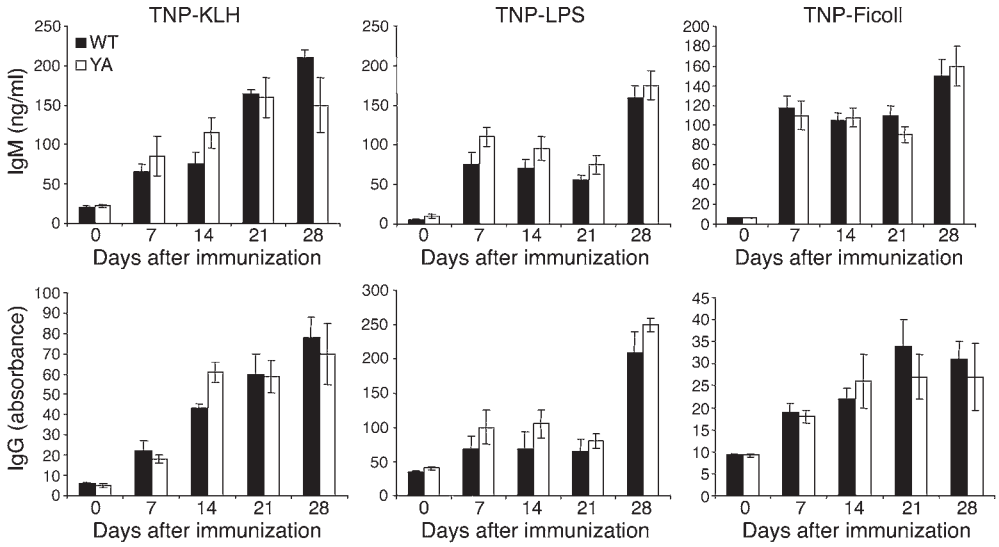

Figure 7
T cell–dependent and –independent humoral immune responses are not impaired by the disruption of the α4 integrin–paxillin interaction. WT and α4(Y991A) mice were immunized intraperitoneally with T cell–dependent antigen (TNP-KLH) and T cell–independent antigens (TNP-LPS and TNP-Ficoll) on day 0 and day 21. Anti-TNP IgM and IgG levels from preimmune serum and serum collected weekly after immunization were determined by enzyme-linked immunosorbent assay with TNP-OVA. Data shown are mean ± SEM of 3–4 mice.

humoral immune response. These data suggest that a new class of agents directed against α4 integrin signaling could widen the therapeutic window of anti–α4 integrin blockade. The mice described here will provide a means to test the effect of inhibition of the α4 integrin–paxillin interaction on experimental models of α4 integrin–mediated human diseases and thereby evaluate the value of this novel form of antiadhesive therapy.

Methods

Generation of α4(Y991A) knock-in mice. A P1 mouse ES cell clone containing at least 24 kb of the α4 integrin gene was isolated from a 129Sv/J mouse library by PCR screening (Genome Systems Inc.). The targeting vector, α4-pFloxIII, is based on the *Cre-loxP* recombination strategy. It consisted of a 4.5-kb, 5′ homologous region and a 0.9-kb, 3′ homologous region (Figure 1A) encompassing exon 28, which encodes the cytoplasmic domain of integrin α4. A thymidine kinase/neomycin (TK/Neo) selection cassette was introduced upstream of exon 28 and flanked by *loxP* sites to allow its excision through the actions of Cre recombinase. The targeted exon was generated by PCR (forward primer, 5′-AGGCAAACATGGGCAAAGTT-3′; reverse primer, 5′-CCCCTGCACTAAGAGTATGTCACAAAATCA-3′). The desired mutation, Y991A, was introduced into exon 28 in conjunction with an additional silent mutation that creates a unique *Eco47III* restriction site. Finally, a *loxP* site was introduced just 3′ of exon 28. The linearized targeting construct was electroporated into R1 ES cells. G418-resistant colonies were selected for 7 days and screened by Southern blotting (Figure 1B). Homologous recombination at the α4 locus introduces a new *BamHI* site. This results in a 4.1-kb targeted band versus the 14.7-kb endogenous band following digestion of genomic DNA with *BamHI* and hybridization to a 3′ external probe. After transfection with pTurboCRE vector (GenBank accession no. AF334827), encoding *Cre* recombinase, and counterselection with ganciclovir for loss of TK, 3 clones containing the desired product (referred to as knock-in clones) were obtained. Those 3 homologous ES cell recombinants containing the desired mutation were identified by PCR analysis (Figure 1C) using primers v (5′-GTCCGTTTGGGAAAATGTGAATAACGTC-3′) as the forward primer and vi (5′-CTTGTTCAACAACATCAAGCATGCATTATC-3′) as the reverse primer. PCR products were obtained at expected size: 2,470 bp for knock-in allele, 2,190 bp for WT allele, and 2,050 bp for by-product allele (i.e., recombination between the 2 extreme *loxP* sites) (Figure 1). These clones were karyotyped, and the best 2 were subsequently injected into E3.5 C57BL/6 host blastocysts. The blastocysts were then transferred into pseudopregnant foster females. A total of 5 chimeric males (distinguished by coat color) were obtained and bred to

Figure 8
The α4 integrin–paxillin interaction is required for optimal organogenesis of Peyer's patches. The number (**A**) and size (**B**) of intestinal Peyer's patches in WT and α4(Y991A) mice are shown. Peyer's patches were identified and enumerated by gross morphology. Peyer's patch diameter was evaluated with a micrometer. Results shown are mean ± SEM of 6–8 mice. **P* = 0.014, 2-tailed Student's *t* test. (**C**) Histology of Peyer's patches from WT and α4(Y991A) is shown. Sections from paraffin embedded intestines were stained with H&E. Arrows indicate Peyer's patches. Magnification, ×100. (**D**) The percentage of T and B cells in Peyer's patches from WT and α4(Y991A) is shown. Cells isolated from Peyer's patches were stained with anti-B220 and anti-CD3 and analyzed by flow cytometry. Results are representative of 6–8 different mice.

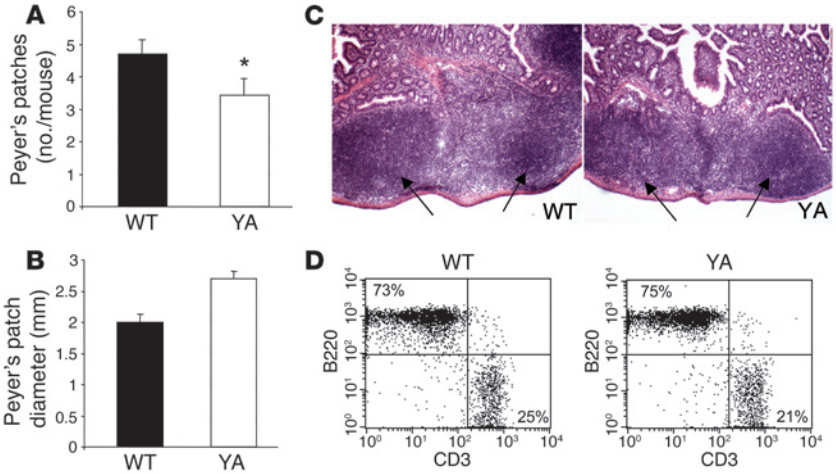

WT C57BL/6 females. Agouti offspring (germline offspring) was genotyped by preparing DNA from tail biopsy for the presence of the targeted allele. Heterozygote males were identified by PCR analysis and ascertained by restriction digests of PCR products using *Eco47III*. Two independent lines were obtained, and genotype was confirmed by Southern blotting on tail biopsies (Figure 1D). All experiments were performed on both lines individually. Mice were housed in the UCSD animal facility, and experiments were approved by the UCSD Institutional Animal Care and Use Committee.

Coimmunoprecipitation and Western blotting. T lymphocytes (4×10^7) obtained from mice and washed in ice-cold PBS were incubated with Sulfo-NHS-biotin (1.1 mg in 5 ml PBS; Pierce Biotechnology Inc.) for 30 minutes at room temperature. Unreacted biotin was quenched and washed from the cells with TBS (0.1 M Tris-HCl, pH 7.4; 150 mM NaCl). Cell lysates were then prepared with lysis buffer (20 mM Tris-HCl, pH 7.4; 150 mM NaCl; 10 mM EDTA; 1% Triton X-100; 0.05% Tween-20; and protease inhibitor cocktail; Roche Diagnostics Corp.). Lysate containing 100 μg protein was immunoprecipitated using 1 μg antibody. Immunoprecipitated proteins were separated by SDS-PAGE (4–20%, denaturing and reducing) gel, transferred to nitrocellulose membrane, and detected using Vectastain ABC kit for biotinylated α4 integrin and ECL for paxillin. Antibodies used were as follows: R1-2 (rat anti-mouse α4; BD Biosciences — Pharmingen), Rb4356 (rabbit anti-paxillin serum generated in the laboratory) (8), mouse monoclonal anti-paxillin (BD Biosciences — Pharmingen), mouse IgG1 (Chemicon International), and rabbit IgG (BioSource International).

Flow cytometry. Cells were harvested from spleen, thymus, and bone marrow and stained with various combinations of the following anti-mouse antibodies obtained from BD Biosciences — Pharmingen: FITC-conjugated anti-CD3 (145-2c11), APC-conjugated anti-CD4 (L3T4/GK1.5), PerCP-conjugated anti-CD8 (Ly2,53-6.7), FITC-conjugated anti-CD21/35 (7G6), PE-conjugated anti-CD23 (B3B4), PerCP-conjugated anti-CD45R/B220 (Ra3-6B2), FITC-conjugated anti-IgD (11-26c.2a), and PE-conjugated anti-IgM (R6-60.2). Cell staining was analyzed with FACScan flow cytometer using CellQuest software (version 3.3; BD Biosciences — Immunocytometry Systems).

Hematology and hematopoiesis. Peripheral blood was collected from the retro-orbital plexus and immediately transferred to tubes containing EDTA. Cell counts were performed using a MS9 automated cell counter with veterinary parameters and reagents. Differential counts were performed manually on Wright-Giemsa–stained smears.

Colony-forming assays and in vivo homing experiments. Marrow cells were obtained from normal and α4(Y991A) mice by flushing as previously described (27), and colony-forming assays were prepared with the following modifications: for GM-CFU and BFU-E cultures, 1×10^5 marrow or 2×10^5 spleen cells were plated in methocult medium (no. M3434; StemCell Technologies) supplemented with 10 μg/ml IL-3, 10 μg/ml IL-6, 50 μg/ml SCF, and 3 U/ml erythropoietin. Cultures were incubated in a fully humidified, 5% CO_2–containing atmosphere at 37°C for 10 days. For CFU-Mk–derived colonies, the marrow cells were instead plated in megacult medium (no. 04960; StemCell Technologies) supplemented with 5 μg/ml IL-3 and 10 μg/ml thrombopoietin. Homing experiments were performed using 2×10^7 marrow cells from the 2 mouse strains injected intraorbitally into C57BL/6 mice irradiated with 9 cGy; marrow and spleen cells were harvested 24 hours after injection for standard colony-forming assays.

Thioglycollate-induced peritonitis. Mice 8–12 weeks old were injected intraperitoneally with 1 ml sterile 4% (wt/vol) thioglycollate (Sigma-Aldrich). At various times after injection, mice were sacrificed and subjected to peritoneal lavage with 4 ml PBS containing 5 mM EDTA and 1% BSA. Total leukocytes in lavage samples were enumerated with a hemocytometer. Cells (1×10^5) were attached to glass slides with a Cytospin4 instrument (ThermoShandon) and stained with modified Wright-Giemsa stain. Differential cell counts were performed on 5 individual fields, each containing 100 cells, by light microscopy. The proportion of T and B lymphocytes in the lavage fluid was determined by flow cytometry using FITC-conjugated anti-CD3 and PerCP-conjugated anti-CD45R/B220 as T and B lymphocyte markers, respectively. B1 and B2 cells were distinguished by relative proportion being $B220^+Mac\text{-}1^+$ and $B220^+Mac\text{-}1^-$, respectively.

Adoptive transfer and assessment of lymphocyte trafficking in thioglycollate-induced peritonitis. Unstimulated splenic lymphocytes were isolated by density gradient centrifugation on Lympholite (Cedarlane Laboratories Ltd.). WT and α4(Y991A) cells were labeled with CFSE and (5/6-[4-chloromethylbenzoyl] aminotetramethylrhodamine) (Invitrogen Corp.), respectively, as previously described (28). Cells were mixed to achieve an approximately 1:1 ratio, and 1×10^8 total cells were injected intravenously into recipient WT and α4(Y991A) mice that had been injected with 1 ml 4% thioglycollate intraperitoneally 4 hours previously as described above. Recipient mice were sacrificed 24 hours after cell transfer, and spleens, blood, peripheral lymph nodes, and peritoneal lavage cells were collected as described above. Flow cytometry was used to evaluate the relative proportion of transferred WT and α4(Y991A) lymphocytes found in recipient organs.

Immunizations and immunoassays. WT and α4(Y991A) mice 8–12 weeks of age of both sexes were immunized intraperitoneally with 100 μg TNP-KLH (Biosearch Technologies Inc.) in complete Freund's adjuvant, 50 μg TNP-LPS (Biosearch Technologies Inc.) in PBS, or 25 μg TNP-Ficoll (Biosearch Technologies Inc.) in PBS on day 0 and boosted on day 21. Blood samples were collected from the retro-orbital sinus on day 0 and weekly through day 28 after immunization. Hapten-specific IgM and IgG levels were quantified in microtiter wells coated with TNP-OVA (Biosearch Technologies Inc.). Bound antibody was detected with HRP-conjugated goat anti-mouse IgM or IgG.

Histology and immunofluorescence. Tissue samples were fixed overnight in 4% formaldehyde and embedded in paraffin. Sections were cut and stained with H&E. Slides were examined with a Leica DM LS microscope and images acquired with a SPOT color digital camera (Diagnostic Instruments).

For immunofluorescence, spleens were frozen in O.C.T. embedding media (Sakura Finetek Co.) and sectioned with a Leica CM3050S Cryostat. Sections were fixed with acetone and double stained for either B220/MOMA1 or IgD/IgM. The antibodies used for B220/MOMA1 were a PE-conjugated rat anti-mouse CD45R/B220 (RA3-6B2) antibody and a rat anti-mouse MOMA-1 antibody (Serotec), which was detected with a FITC-goat polyclonal anti-rat IgG antibody (Jackson ImmunoResearch Laboratories Inc.). The antibodies used for IgD/IgM were FITC-conjugated rat anti-mouse IgD and PE-conjugated rat anti-mouse IgM (BD Biosciences — Pharmingen). Slides were examined on a Leica DM LS fluorescent microscope, and images were acquired as described above.

Statistics. Data were analyzed for statistical significance using the 1- or 2-tailed Student's *t* test. *P* values less than 0.05 were considered significant.

Acknowledgments

We gratefully acknowledge Marina Slepak for her excellent technical assistance. This work was supported by grants from the NIH. C.C. Féral is a postdoctoral fellow, and D.M. Rose and J. Han are Arthritis Investigators of the Arthritis Foundation.

Received for publication June 28, 2005, and accepted in revised form December 13, 2005.

Address correspondence to: Mark H. Ginsberg, Department of Medicine, University of California San Diego, 9500 Gilman Drive, Mail Stop 0726, La Jolla, California 92093-0726, USA. Phone: (858) 822-6432; Fax: (858) 822-6458; E-mail: mhginsberg@ucsd.edu.

Chloé C. Féral and David M. Rose contributed equally to this work.

1. Ransohoff, R.M., Kivisakk, P., and Kidd, G. 2003. Three or more routes for leukocyte migration into the central nervous system. *Nat. Rev. Immunol.* **3**:569–581.
2. Smolen, J.S., and Steiner, G. 2003. Therapeutic strategies for rheumatoid arthritis. *Nat. Rev. Drug Discov.* **2**:473–488.
3. James, W.G., Bullard, D.C., and Hickey, M.J. 2003. Critical role of the alpha 4 integrin/VCAM-1 pathway in cerebral leukocyte trafficking in lupus-prone MRL/fas(lpr) mice. *J. Immunol.* **170**:520–527.
4. von Andrian, U.H., and Engelhardt, B. 2003. Alpha4 integrins as therapeutic targets in autoimmune disease. *N. Engl. J. Med.* **348**:68–72.
5. Miller, D.H., et al. 2003. A controlled trial of natalizumab for relapsing multiple sclerosis. *N. Engl. J. Med.* **348**:15–23.
6. Arroyo, A.G., Yang, J.T., Rayburn, H., and Hynes, R.O. 1996. Differential requirements for α4 integrins in hematopoiesis. *Cell.* **85**:997–1008.
7. Sheridan, C. 2005. Third tysabri adverse case hits drug class. *Nat. Rev. Drug Discov.* **4**:357–358.
8. Rose, D.M., et al. 2003. Paxillin binding to the alpha 4 integrin subunit stimulates LFA-1 (Integrin alpha L beta 2)-dependent T Cell migration by augmenting the activation of focal adhesion kinase/proline-rich tyrosine kinase-2. *J. Immunol.* **170**:5912–5918.
9. Ylanne, J., et al. 1993. Distinct functions of integrin α and β subunit cytoplasmic domains in cell spreading and formation of focal adhesions. *J.Cell Biol.* **122**:223–233.
10. Rose, D.M., Grabovsky, V., Alon, R., and Ginsberg, M.H. 2001. The affinity of integrin alpha 4 beta 1 governs lymphocyte migration. *J. Immunol.* **167**:2824–2830.
11. Liu, S., et al. 1999. Paxillin binding to alpha 4 integrins modifies integrin-dependent biological responses. *Nature.* **402**:676–681.
12. Liu, S., et al. 2002. A fragment of paxillin binds the alpha 4 integrin cytoplasmic domain (tail) and selectively inhibits alpha 4-mediated cell migration. *J. Biol. Chem.* **277**:20887–20894.
13. Ambroise, Y., Yaspan, B., Ginsberg, M.H., and Boger, D.L. 2002. Inhibitors of cell migration that inhibit intracellular paxillin/alpha4 binding. A well-documented use of positional scanning libraries. *Chem. Biol.* **9**:1219–1226.
14. Yang, J.T., Rayburn, H., and Hynes, R.O. 1995. Cell adhesion events mediated by alpha 4 integrins are essential in placental and cardiac development. *Development.* **121**:549–560.
15. Scott, L.M., Priestley, G.V., and Papayannopoulou, T. 2003. Deletion of alpha 4 integrins from adult hematopoietic cells reveals roles in homeostasis, regeneration, and homing. *Mol.Cell. Biol.* **23**:9350–9361.
16. Arroyo, A.G., Yang, J.T., Rayburn, H., and Hynes, R.O. 1999. Alpha 4 integrins regulate the proliferation/differentiation balance of multilineage hematopoietic progenitors in vivo. *Immunity.* **11**:555–566.
17. Papayannopoulou, T., and Craddock, C. 1997. Homing and trafficking of hemopoietic progenitor cells. *Acta Haematol.* **97**:97–104.
18. Oostendorp, R.A., Ghaffari, S., and Eaves, C.J. 2000. Kinetics of in vivo homing and recruitment into cycle of hematopoietic cells are organ-specific but CD44-independent. *Bone Marrow Transplant.* **26**:559–566.
19. Lo, C.G., Lu, T.T., and Cyster, J.G. 2003. Integrin-dependence of lymphocyte entry into the splenic white pulp. *J. Exp. Med.* **197**:353–361.
20. Lu, T.T., and Cyster, J.G. 2002. Integrin-mediated long-term B cell retention in the splenic marginal zone. *Science.* **297**:409–412.
21. Sengbusch, J.K., He, W., Pinco, K.A., and Yang, J.T. 2002. Dual functions of alpha 4 beta 1 integrin in epicardial development: initial migration and long-term attachment. *J. Cell Biol.* **157**:873–882.
22. Young, B.A., et al. 2001. The cytoplasmic domain of the integrin alpha 9 subunit requires the adaptor protein paxillin to inhibit cell spreading but promotes cell migration in a paxillin-independent manner. *Mol. Biol. Cell.* **12**:3214–3225.
23. Finke, D., Acha-Orbea, H., Mattis, A., Lipp, M., and Kraehenbuhl, J. 2002. CD4+CD3- cells induce Peyer's patch development: role of alpha 4 beta 1 integrin activation by CXCR5. *Immunity.* **17**:363–373.
24. Finke, D., and Kraehenbuhl, J.P. 2001. Formation of Peyer's patches. *Curr. Opin. Genet. Dev.* **11**:561–567.
25. Hyduk, S.J., Oh, J., Xiao, H., Chen, M., and Cybulsky, M.I. 2004. Paxillin selectively associates with constitutive and chemoattractant-induced high-affinity alpha 4 beta 1 integrins: implications for integrin signaling. *Blood.* **104**:2818–2824.
26. Quinn, M.J., Plow, E.F., and Topol, E.J. 2002. Platelet glycoprotein IIb/IIIa inhibitors: recognition of a two-edged sword? *Circulation.* **106**:379–385.
27. Kaushansky, K., et al. 1995. Thrombopoietin expands erythroid progenitors, increases red cell production, and enhances erythroid recovery after myelosuppressive therapy. *J. Clin. Invest.* **96**:1683–1687.
28. Goodyear, C.S., and Silverman, G.J. 2003. Death by a B cell superantigen: in vivo VH-targeted apoptotic supraclonal B cell deletion by a Staphylococcal toxin. *J. Exp. Med.* **197**:1125–1139.